

# Photoinduced Solid–Liquid Phase Transition and Energy Storage Enabled by the Design of Linked Double Photoswitches

Alejandra Gonzalez, Qianfeng Qiu, Junichi Usuba, Joshua Wan, and Grace G. D. Han\*

Cite This: *ACS Mater. Au* 2024, 4, 30–34

Read Online

ACCESS |

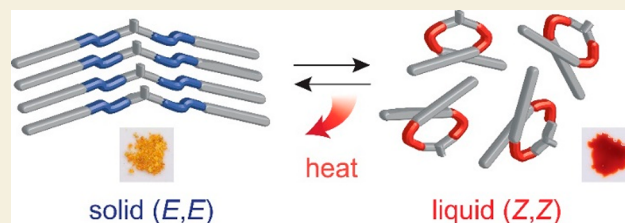
Metrics &amp; More

Article Recommendations

Supporting Information

**ABSTRACT:** We demonstrate an effective design strategy of photoswitchable phase change materials based on the bis-azobenzene scaffold. These compounds display a solid phase in the *E,E* state and a liquid phase in the *Z,Z* state, in contrast to their monoazobenzene counterparts that exhibit less controlled phase transition behaviors that are largely influenced by their functional groups.

**KEYWORDS:** Azobenzenes, Phase Transition, Energy Storage, Isomerization, Photoswitches



Photoinduced phase transition of photoswitches between solid and liquid has recently emerged as a strategy that effectively increases the total energy storage density of molecular solar thermal energy storage (MOST) systems.<sup>1–4</sup> In particular, photoswitches including azobenzene<sup>5–8</sup> and azoheteroarene<sup>9,10</sup> derivatives that undergo large structural changes upon *E*–*Z* isomerization have been primarily investigated for drastic phase transitions. *E* isomers generally exhibit a planar molecular structure that forms a crystalline phase, whereas *Z* isomers display a twisted<sup>11,12</sup> or T-shaped<sup>13</sup> geometry that is less prone to crystallization at room temperature and forms a liquid phase under ambient conditions. A generally established design of such molecules for MOST applications involves a photoswitch core, azobenzene or azoheteroarene, and a *p*-substituent (Figure 1a) that ranges from a small methoxy or ethoxy group<sup>14</sup> to longer alkyl chains.<sup>10,15–17</sup> However, achieving distinct phases of *E* and *Z* isomers remains a challenge due to the inconsistencies in the properties displayed by each functionalization and thus requires extensive screening of small substituents, the length of alkyl chains, and the structure of photoswitch cores to find suitable molecular structures.

For example, *p*-substitution of azobenzene with functional groups including F, Cl, Br, I, CN, and NO<sub>2</sub><sup>14</sup> result in the formation of solid phase for both *E* and *Z* isomers, due to the facile crystallization of twisted *Z* structures. Out of a large series of arylazopyrazole derivatives *p*-substituted on the aryl ring with various alkoxy groups (OC<sub>*n*</sub>H<sub>2*n*+1</sub> and OC<sub>*n*</sub>H<sub>2*n*-1</sub>; *n* = 1–12),<sup>1</sup> only one compound (OC<sub>8</sub>H<sub>15</sub>) displays a liquid phase as *Z* isomer (i.e., melting point below room temperature), while the rest of the compounds with shorter or longer chains are solids as both *E* and *Z* isomers. The phase of *Z* isomer is also impacted by the *o*-substituents on azobenzene core;<sup>18</sup> for example, azobenzenes *o*-substituted with halides (F and Cl) undergo solid–liquid phase transition, while the *o*-MeO-

substituted azobenzene exhibits solid phases for both *E* and *Z*, despite bearing an identical *p*-tridecanoate group. Other examples include alkyl-functionalized ionic crystal–liquid azobenzene derivatives,<sup>5</sup> azobispyrazoles,<sup>9</sup> and hydrazones,<sup>19</sup> which reveal the challenges of controlling the phase of photoisomer that is sensitive to both the chain lengths and the type of counter-anions.

These examples highlight the critical need to develop more generalizable and robust design principles of phase-transition MOST compounds that present crystalline *E* and liquid *Z* phases. One potential candidate is a multiphotoswitch system that incorporates two or more azoarene moieties, which is anticipated to maximize the structural difference between the planar *E* and nonplanar *Z* isomers. Multiazoarene systems have been previously investigated in solutions,<sup>20,21</sup> and their light-responsive behaviors in gels<sup>22</sup> and polymer matrices<sup>23,24</sup> have been reported. Importantly, the photoinduced melting of crystalline multiazoarene compounds,<sup>25–29</sup> which was primarily employed for the photocontrolled adhesion, gas uptake, and catalysis, unveils the potential of such designs for the successful development of phase-transition MOST systems.

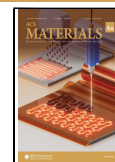
Herein, we report a series of MOST compounds (Figure 1b) that connect two azobenzenes by a short linkage, exhibiting distinct solid and liquid phases as *E* and *Z* isomers, independent of the length or rigidity of terminal groups (H, octyl, and perfluorooctyl; compounds 1–3) that typically challenge such phase transition in azobenzene designs. We

Received: August 28, 2023

Revised: September 19, 2023

Accepted: September 22, 2023

Published: September 26, 2023



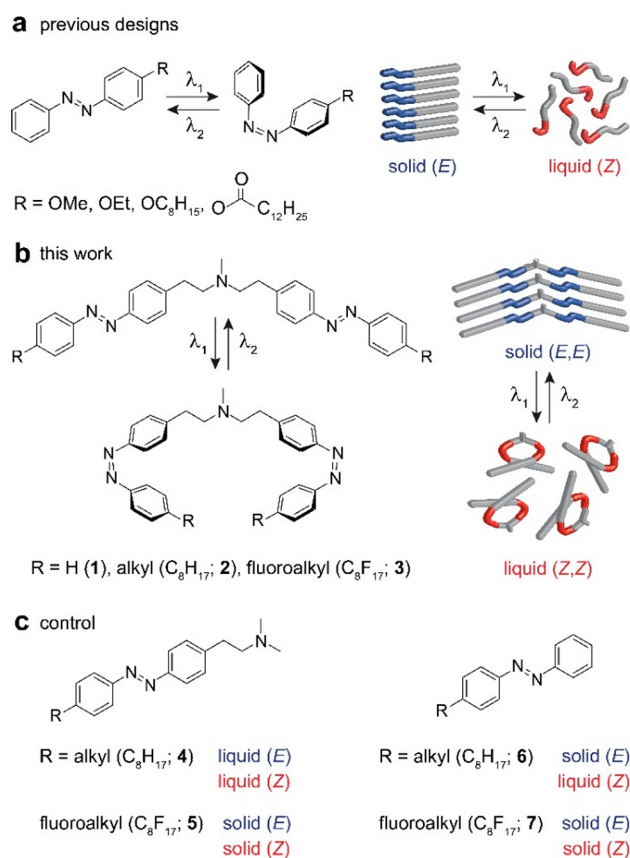


**Figure 1.** (a) Azobenzene derivatives that are reported to exhibit solid–liquid phase transition upon reversible photoisomerization. (b) Design of symmetric photoswitches bearing two azobenzene moieties and varied terminal groups, which allows for solid–liquid phase transition. (c) Design of azobenzene derivatives with *p*-substituent(s) that serve for control experiments.

investigate the importance of symmetrical molecular designs by comparing the phase behavior of asymmetrical, monoazobenzene counterparts (Figure 1c) that are functionalized with the identical terminal groups. Compounds 4 and 5 are substituted with an octyl and perfluoroctyl group, respectively, and both are designed to retain the terminal tertiary amine group on the opposite *p*-position to examine the presence of intramolecular interactions between two *p*-substituents. Compounds 6 and 7 bear an octyl and perfluoroctyl group, respectively, on the *p*-position, which eliminates the impact of the terminal amine group on molecular packing as *E* or *Z* isomers. As the summary of their phase behavior indicates, it is extremely challenging to predict and achieve the desired solid (*E*) and liquid (*Z*) phases of monoazobenzene scaffold, which underlines the efficacy of bis-azobenzene designs that yield such phase difference even in the presence of large London dispersion and fluororous interactions. We note that *Z*-rich samples with maximum photostationary state (PSS) ratios were prepared in solutions and then condensed by leveraging the facile and rapid *E*-to-*Z* isomerization in solution state.

Our bis-azobenzene compounds 1–3 are connected by a diethylmethylamine linker, which was primarily selected for the synthetic ease of reductive amination that enables coupling of two azobenzene units. The linkage also serves to electronically decouple<sup>30</sup> the photoswitching units and retain the desirable optical and switching properties of azobenzene. Also, a small linkage moiety is desired to achieve large energy storage

densities. Synthesis, NMR, and HRMS characterization of all compounds are in the Supporting Information (Schemes S1–S4, Figures S1–S28). To confirm the validity of the conceived symmetric molecular design, X-ray crystallography of single crystals of 1-*E,E* grown from ethyl acetate and diethyl ether was performed. 1-*E,E* adopts a conformation in which a pair of planar azobenzene moieties are arranged in a V-shape with an angle of 108° (Figure S29). The V-shaped molecules stack in 1D columns and exhibit offset  $\pi$ -stacking among neighboring azobenzene units (Figure 2a). Since the other compounds

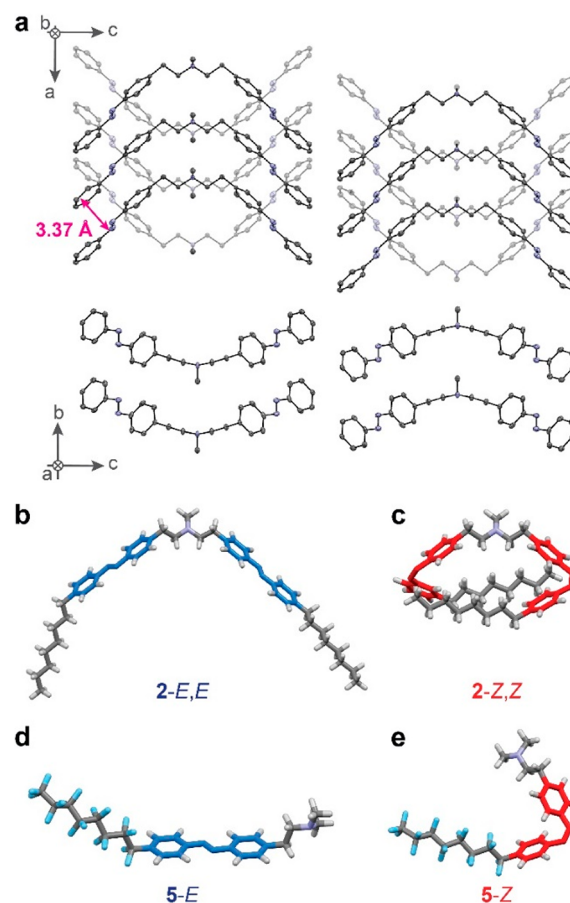


**Figure 2.** (a) Crystal structure and packing of 1-*E,E* in the thermal ellipsoid at 50% probability. The hydrogen atoms are omitted for clarity. Optimized structures of (b) 2-*E,E*, (c) 2-*Z,Z*, (d) 5-*E*, and (e) 5-*Z* calculated at the B3LYP/6-31+G(d,p) level of theory.

were unable to form high quality crystals suitable for single crystal X-ray crystallography, DFT calculations were performed to predict their structures (Figures S30–S36). The optimized V-shaped geometry of the core structure in 2-*E,E* (Figures 2b, S31) and 3-*E,E* (Figure S33) is consistent with the crystal structure of 1-*E,E*. Thus, we hypothesize that these compounds would also form 1D columnar packing in the solid state. In contrast, the DFT-optimized *Z,Z* isomers display an overall circular shape consisting of two twisted azobenzene units and two linear side chains that are not aligned to each other (Figures 2c, S32). Based on the nonlinear, 3D circular structure, the *Z,Z* isomers are anticipated not to form crystalline packing in the absence of any favorable intermolecular  $\pi$  interactions or London dispersion force. The structures of compounds 4 and 5 in both *E* and *Z* isomeric states were also optimized by DFT (Figures S35, S36),

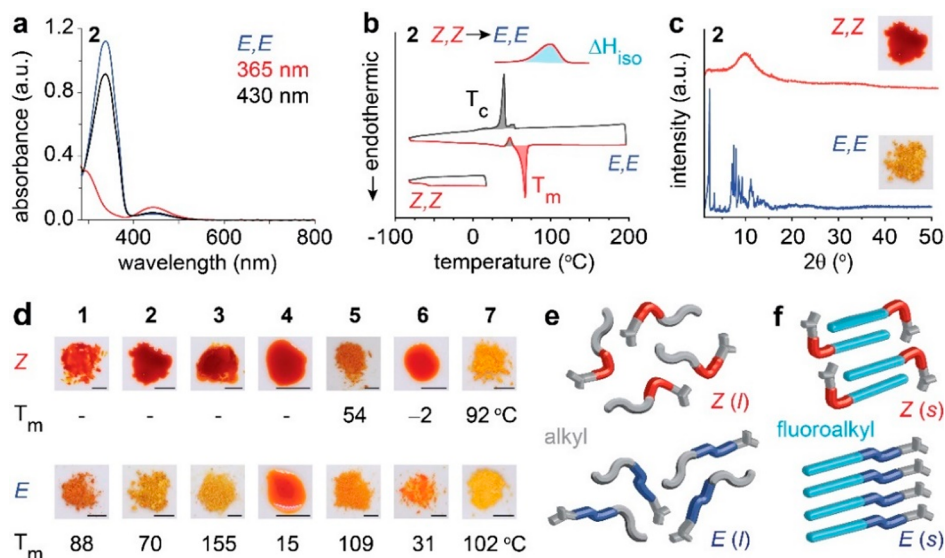


**Figure 3.** (a) UV-vis absorption spectra, (b) DSC plots, and (c) PXRD patterns of compound 2 as *E* and *Z* isomers.  $T_m$ : melting point,  $T_c$ : crystallization point,  $\Delta H_{iso}$ : isomerization energy. (d) Optical images of all compounds as *E* and *Z* isomers and their  $T_m$  measured by DSC.  $T_m$  of compounds 1–4 *Z* could not be detected by DSC. Schematic illustrations of *E* and *Z* isomers in condensed phases for compounds (e) 4 and (f) 5.

showing planar *E* (Figure 2d) and bent *Z* (Figure 2e) cores and linear chains attached to the core structures for compound 5. Similar structures of compound 4 are displayed in Figure S35. Cartesian coordinates for optimized geometries are available in the Supporting Information (Tables S2–S12).

All synthesized compounds display similar absorption profiles as pristine azobenzene, featuring a  $\pi-\pi^*$  band around 340 nm and a  $n-\pi^*$  band around 430 nm for *E* isomers and the blue-shifted  $\pi-\pi^*$  band upon switching to *Z* isomers, as shown in Figures 3a and S37. In bis-azobenzene derivatives, each azobenzene unit is electronically isolated from each other due to the presence of an *N,N*-diethylmethylamine linker. At the PSS under irradiation of 365 nm in solution, nearly 100% of *E*  $\rightarrow$  *Z* conversion was achieved, and 77% of *Z*  $\rightarrow$  *E* isomerization was observed under irradiation of 430 nm (Figure S38). Compounds 1–3 bearing two azobenzene groups show distinct phases, i.e., crystalline *E,E* and liquid *Z,Z* at room temperature, as confirmed by differential scanning calorimetry (DSC) (Figure S39). Figure 3b shows an example of such phase characteristics of compound 2, which features a set of melting and crystallization peaks for the *E,E* isomer and the lack of those for the *Z,Z* counterpart. The *Z,Z* isomer exhibits an extreme liquid stability even at subzero temperatures as low as  $-80$  °C that is the measurement limit of DSC. The *Z,Z* state undergoes a thermally induced reverse isomerization to *E,E*, releasing the isomerization energy ( $\Delta H_{iso}$ ) above 68 °C. The summary of DSC parameters for all compounds is provided in Table S13. Such a phase difference between two isomeric states is also corroborated by the powder X-ray diffraction of solid *E,E* and liquid *Z,Z*, showing distinct diffraction peaks for *E,E* and the amorphous nature of *Z,Z* (Figure 3c). The *E*–*Z* diffraction patterns of all compounds are included in Figure S40.

Compared to bis-azobenzenes 1–3, the monoazobenzene derivatives 4–7 exhibit less predictable phase differences between the *E* and *Z* isomers (Figure 3d). Indeed, whereas compounds 1–3 exhibit a solid phase for *E,E* and a liquid phase for *Z,Z* independent of functional groups, phases of *E* and *Z* isomers of compounds 4–7 are largely influenced by

their functional groups. *p*-Octyl-functionalized compound 4 exhibits liquid phase for both *E* and *Z* at room temperature, due to the large disorder of the flexible alkyl functional group (Figure 3e). In contrast, compound 5 with a *p*-perfluorooctyl substituent forms a crystalline state for both *E* and *Z*, as a result of the strong intermolecular fluororous interactions between the rigid perfluorooctyl chains (Figure 3f). It is predicted that intramolecular interactions between the *p*-octyl (or perfluorooctyl) and *p*-*N,N*-dimethylethylamine groups in *Z* isomers are insignificant based on the DFT calculations of stable *Z* conformations (Figures S35, S36) and NOESY NMR analysis (Figures S41, S42). In addition, the presence of the terminal amine group does not impact the *Z* stability, which is verified by the *Z* thermal half-life measurements showing the similar half-lives of compounds 1–7 spanning 1 to 3 days (Figures S43–S49).

However, the flexibility of the *N,N*-dimethylethylamine group contributes to the disorder of monoazobenzene compound 4-*E* that displays a melting point ( $T_m$ ) below room temperature (15 °C). Eliminating the flexible amine group thus raised the  $T_m$  of compound 6-*E* to 16 °C, resulting in a waxy solid state at room temperature. The comparison between compounds 4 and 6 highlights the challenges in achieving desired phases of monoazobenzene derivatives, which significantly depends on the subtle changes in chemical structures and their flexibility, such as the chain length and functional groups. The *p*-perfluorooctyl-functionalized compound 7 shows crystalline state for both *E* and *Z*, similar to compound 5, which emphasizes the lower disorder of perfluoroalkyl chains and their rigidity that yield crystalline packing of monoazobenzene derivatives. The impact of alkyl and perfluoroalkyl chains on condensed-phase packing is also confirmed by the lowered and raised  $T_m$  of *E* isomers, e.g., 70 °C (2) vs 155 °C (3), 15 °C (4) vs 109 °C (5), and 31 °C (6) vs 102 °C (7). Despite the presence of two perfluorooctyl groups in compound 3, the bis-azobenzene scaffold produces a liquid state upon 340 nm irradiation, within a large window of temperature (i.e.,  $-80$  to 57 °C, Figure S39), which is

governed by the remarkably twisted, nonplanar structure of the *Z,Z* configuration.

As a result of the different phase behaviors, the total energy storage density ( $\Delta H_{\text{total}}$ ) in each MOST compound is varied. The solid–liquid MOST systems (Figure 4a) store the largest

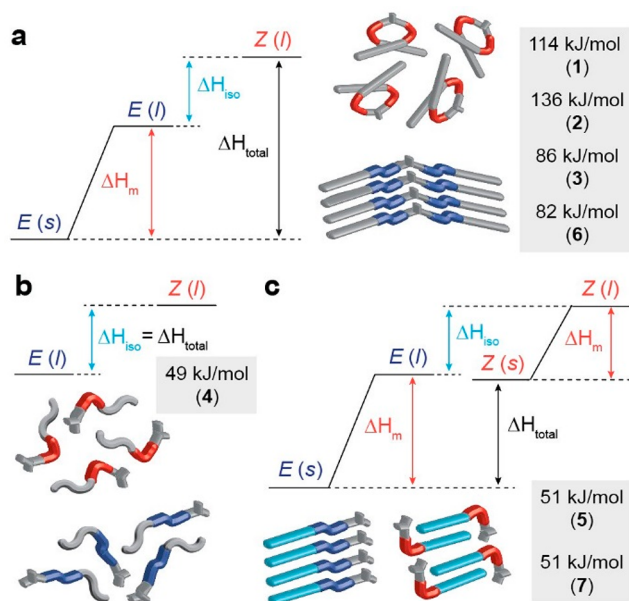


**Figure 4.** Energy diagrams of phase change and isomerization for three classes of compounds that undergo (a) solid–liquid, (b) liquid–liquid, and (c) solid–solid transitions upon photoisomerization and the total energy storage density ( $\Delta H_{\text{total}}$ ) of each compound.

amount of energy in the *Z*-rich state, combining  $\Delta H_{\text{iso}}$  and phase transition enthalpy, or the melting enthalpy ( $\Delta H_{\text{m}}$ ) of the *E,E* (or *E*) isomer. The larger  $\Delta H_{\text{total}}$  of compound 2 compared to that of 1 is primarily attributed to the larger  $\Delta H_{\text{m}}$  of 2-*E,E* (51 kJ/mol) than that of 1-*E,E* (35 kJ/mol) (Table S13). Due to the large London dispersion of the octyl chains that increases the phase transition energy, compound 2 displays the largest  $\Delta H_{\text{total}}$  of 136 kJ/mol, which equates to 68 kJ/mol per azobenzene unit. The perfluorooctyl-substituted bisazobenzene 3, however, shows a greatly reduced  $\Delta H_{\text{total}}$  of 86 kJ/mol. The accurate quantification of  $\Delta H_{\text{iso}}$  for compound 3 is challenging, because of the significant overlap between the *Z* → *E* thermal reversion, the crystallization of the formed *E,E* isomers, and the subsequent melting of *E,E* (Figure S39), which may result in the underestimation of  $\Delta H_{\text{iso}}$ . Compound 6 shows an overall large  $\Delta H_{\text{total}}$  of 82 kJ/mol, despite the narrow range of temperature that allows for the solid–liquid phase transition, which is limited by the  $T_{\text{m}}$  of *Z* at  $-2$  °C and that of *E* at 31 °C.

Compound 4 that undergoes isomerization in a condensed liquid can store only  $\Delta H_{\text{iso}}$  (49 kJ/mol) and no phase transition enthalpy (Figure 4b). Compounds 5 and 7 that form crystalline phases for both *E* and *Z* can store  $\Delta H_{\text{iso}}$  and the crystal-to-crystal phase transition enthalpy that is calculated by the difference between  $\Delta H_{\text{m}}$  (*E*) and  $\Delta H_{\text{m}}$  (*Z*) (Figure 4c). The  $\Delta H_{\text{total}}$  values of compounds 5 and 7 (51 kJ/mol) are similar to that of compound 4, revealing the unique advantage of solid–liquid phase-transition MOST compounds illustrated in Figure 4a in achieving larger  $\Delta H_{\text{total}}$ . In addition, we note that  $\Delta H_{\text{iso}}$  values obtained for bis-azobenzene compounds 1–3 are less than twice the  $\Delta H_{\text{iso}}$  of monoazobenzene compounds

4–7 (Table S13). We hypothesize that intramolecular interactions within the circular *Z,Z* configurations could stabilize the metastable state isomers, thus reducing the energy gap between the thermodynamically stable *E,E* and metastable *Z,Z* states, which translates to smaller  $\Delta H_{\text{iso}}$  values.

In summary, a series of bis-azobenzene compounds was systematically investigated to elucidate the significance of multiphotoswitch design and symmetry of molecule on achieving distinct solid and liquid phases upon isomerization. In contrast to their monoazobenzene analogues, bis-azobenzene compounds exhibit predictable solid and liquid phase characteristics for *E,E* and *Z,Z* states, respectively, regardless of the rigidity of functional groups on photochromes. This is primarily due to the high planarity and symmetry of the *E,E* state and the largely disordered and circular geometry of the *Z,Z* state. These results offer an effective strategy for controlling the phase of MOST compounds and maximizing their energy storage densities, which may be broadly applicable to other *E*–*Z* photoswitches for energy applications.

## ■ ASSOCIATED CONTENT

### Supporting Information

The Supporting Information is available free of charge at <https://pubs.acs.org/doi/10.1021/acsmaterialsau.3c00069>.

Methods, synthesis, single crystal XRD data, DFT calculation results, UV–vis spectra, DSC plots, PXRD data, kinetic analysis, and supplementary figures (PDF)

## ■ AUTHOR INFORMATION

### Corresponding Author

Grace G. D. Han – Department of Chemistry, Brandeis University, Waltham, Massachusetts 02453, United States; [orcid.org/0000-0002-2918-1584](https://orcid.org/0000-0002-2918-1584); Email: [gracehan@brandeis.edu](mailto:gracehan@brandeis.edu)

### Authors

Alejandra Gonzalez – Department of Chemistry, Brandeis University, Waltham, Massachusetts 02453, United States;

[orcid.org/0000-0001-6483-5005](https://orcid.org/0000-0001-6483-5005)

Qianfeng Qiu – Department of Chemistry, Brandeis University, Waltham, Massachusetts 02453, United States

Junichi Usuba – Department of Chemistry, Brandeis University, Waltham, Massachusetts 02453, United States

Joshua Wan – Department of Chemistry, Brandeis University, Waltham, Massachusetts 02453, United States

Complete contact information is available at:

<https://pubs.acs.org/doi/10.1021/acsmaterialsau.3c00069>

### Author Contributions

CRediT: Alejandra Gonzalez investigation, writing-original draft; Qianfeng Qiu investigation, writing-review & editing; Junichi Usuba data curation, formal analysis, visualization, writing-review & editing; Joshua Wan investigation, writing-review & editing; Grace G. D. Han conceptualization, formal analysis, funding acquisition, supervision, writing-original draft.

### Notes

The authors declare no competing financial interest.

## ACKNOWLEDGMENTS

This material is based upon work supported by the Air Force Office of Scientific Research under Award Number FA9550-22-1-0254. G.G.D.H. acknowledges the NSF CAREER award (DMR-2142887) and Alfred P. Sloan Foundation (FG-2022-18328). A.G. and J.W. were supported by Brandeis MRSEC (DMR-2011846) and SMURF Program. The authors greatly appreciate Dr. Xiang Li and Han Nguyen for the collection of PXRD patterns.

## REFERENCES

- (1) Hu, J.; Song, T.; Yu, M.-M.; Yu, H. Optically Controlled Solid-to-Liquid Phase Transition Materials Based on Azo Compounds. *Chem. Mater.* **2023**, *35* (12), 4621–4648.
- (2) Li, X.; Cho, S.; Wan, J.; Han, G. G. D. Photoswitches and Photochemical Reactions for Optically Controlled Phase Transition and Energy Storage. *Chem.* **2023**, *9*, 2378.
- (3) Cai, F.; Song, T.; Yang, B.; Lv, X.; Zhang, L.; Yu, H. Enhancement of Solar Thermal Fuel by Microphase Separation and Nanoconfinement of a Block Copolymer. *Chem. Mater.* **2021**, *33* (24), 9750–9759.
- (4) Le, M.; Han, G. G. D. Stimuli-Responsive Organic Phase Change Materials: Molecular Designs and Applications in Energy Storage. *Acc. Mater. Res.* **2022**, *3* (6), 634–643.
- (5) Ishiba, K.; Morikawa, M.; Chikara, C.; Yamada, T.; Iwase, K.; Kawakita, M.; Kimizuka, N. Photoliquefiable Ionic Crystals: A Phase Crossover Approach for Photon Energy Storage Materials with Functional Multiplicity. *Angew. Chem., Int. Ed.* **2015**, *54* (5), 1532–1536.
- (6) Yang, Y.; Huang, S.; Ma, Y.; Yi, J.; Jiang, Y.; Chang, X.; Li, Q. Liquid and Photoliquefiable Azobenzene Derivatives for Solvent-free Molecular Solar Thermal Fuels. *ACS Appl. Mater. Interfaces* **2022**, *14* (31), 35623–35634.
- (7) Huang, X.; Shangquan, Z.; Zhang, Z.-Y.; Yu, C.; He, Y.; Fang, D.; Sun, W.; Li, Y.-C.; Yuan, C.; Wu, S.; Li, T. Visible-Light-Induced Reversible Photochemical Crystal-Liquid Transitions of Azo-Switches for Smart and Robust Adhesives. *Chem. Mater.* **2022**, *34* (6), 2636–2644.
- (8) Kelly, E. A.; Willis-Fox, N.; Houston, J. E.; Blayo, C.; Divitini, G.; Cowieson, N.; Daly, R.; Evans, R. C. A Single-Component Photorheological Fluid with Light-responsive Viscosity. *Nanoscale* **2020**, *12* (11), 6300–6306.
- (9) Gonzalez, A.; Odaybat, M.; Le, M.; Greenfield, J. L.; White, A. J. P.; Li, X.; Fuchter, M. J.; Han, G. G. D. Photocontrolled Energy Storage in Azobispyrazoles with Exceptionally Large Light Penetration Depths. *J. Am. Chem. Soc.* **2022**, *144* (42), 19430–19436.
- (10) Gerkman, M. A.; Gibson, R. S. L.; Calbo, J.; Shi, Y.; Fuchter, M. J.; Han, G. G. D. Arylazopyrazoles for Long-Term Thermal Energy Storage and Optically Triggered Heat Release below 0 °C. *J. Am. Chem. Soc.* **2020**, *142* (19), 8688–8695.
- (11) Bandara, H. M.; Burdette, S. C. Photoisomerization in Different Classes of Azobenzene. *Chem. Soc. Rev.* **2012**, *41* (5), 1809–1825.
- (12) Adrion, D. M.; Lopez, S. A. Cross-conjugation Controls the Stabilities and Photophysical Properties of Heteroazoarene Photoswitches. *Org. Biomol. Chem.* **2022**, *20* (30), 5989–5998.
- (13) Calbo, J.; Weston, C. E.; White, A. J.; Rzepa, H. S.; Contreras-Garcia, J.; Fuchter, M. J. Tuning Azoheteroarene Photoswitch Performance through Heteroaryl Design. *J. Am. Chem. Soc.* **2017**, *139* (3), 1261–1274.
- (14) Qiu, Q.; Gerkman, M. A.; Shi, Y.; Han, G. G. D. Design of Phase-transition Molecular Solar Thermal Energy Storage Compounds: Compact Molecules with High Energy Densities. *Chem. Commun.* **2021**, *57* (74), 9458–9461.
- (15) Zhang, Z. Y.; He, Y.; Wang, Z.; Xu, J.; Xie, M.; Tao, P.; Ji, D.; Moth-Poulsen, K.; Li, T. Photochemical Phase Transitions Enable Coharvesting of Photon Energy and Ambient Heat for Energetic Molecular Solar Thermal Batteries That Upgrade Thermal Energy. *J. Am. Chem. Soc.* **2020**, *142* (28), 12256–12264.
- (16) Kwaria, D.; McGehee, K.; Liu, S.; Kikkawa, Y.; Ito, S.; Norikane, Y. Visible-Light-Photomeltable Azobenzenes as Solar Thermal Fuels. *ACS Appl. Opt. Mater.* **2023**, *1* (2), 633–639.
- (17) Liu, H.; Feng, Y.; Feng, W. Alkyl-grafted Azobenzene Molecules for Photo-induced Heat Storage and Release via Integration Function of Phase Change and Photoisomerization. *Compos. Commun.* **2020**, *21*, 100402.
- (18) Shi, Y.; Gerkman, M. A.; Qiu, Q.; Zhang, S.; Han, G. G. D. Sunlight-activated Phase Change Materials for Controlled Heat Storage and Triggered Release. *J. Mater. Chem. A* **2021**, *9* (15), 9798–9808.
- (19) Qiu, Q.; Yang, S.; Gerkman, M. A.; Fu, H.; Aprahamian, I.; Han, G. G. D. Photon Energy Storage in Strained Cyclic Hydrazones: Emerging Molecular Solar Thermal Energy Storage Compounds. *J. Am. Chem. Soc.* **2022**, *144* (28), 12627–12631.
- (20) Kunz, A.; Heindl, A. H.; Dreos, A.; Wang, Z.; Moth-Poulsen, K.; Becker, J.; Wegner, H. A. Intermolecular London Dispersion Interactions of Azobenzene Switches for Tuning Molecular Solar Thermal Energy Storage Systems. *ChemPlusChem.* **2019**, *84* (8), 1145–1148.
- (21) Kunz, A.; Oberhof, N.; Scherz, F.; Martins, L.; Dreu, A.; Wegner, H. A. Azobenzene-Substituted Triptycenes: Understanding the Exciton Coupling of Molecular Switches in Close Proximity. *Chem.—Eur. J.* **2022**, *28* (38), No. e202200972.
- (22) Zhou, Y.; Xu, M.; Wu, J.; Yi, T.; Han, J.; Xiao, S.; Li, F.; Huang, C. J. A Novel Photo-responsive Organogel Based on Azobenzene. *Phys. Org. Chem.* **2008**, *21* (4), 338–343.
- (23) Vapaavuori, J.; Goulet-Hanssens, A.; Heikkinen, I. T. S.; Barrett, C. J.; Priimagi, A. Are Two Azo Groups Better than One? Investigating the Photoresponse of Polymer-Bisazobenzene Complexes. *Chem. Mater.* **2014**, *26* (17), 5089–5096.
- (24) Audorff, H.; Walker, R.; Kador, L.; Schmidt, H. W. Holographic Investigations of Azobenzene-containing Low-molecular-weight Compounds in Pure Materials and Binary Blends with Polystyrene. *Chem.—Eur. J.* **2011**, *17* (45), 12722–12728.
- (25) Gupta, D.; Gaur, A. K.; Kaur, R.; Ashish; Kaur, N.; Venkataramani, S. Photoswitchable Azoheteroarene-Based Chelating Ligands: Light Modulation of Properties, Aqueous Solubility and Catalysis. *Chem.—Eur. J.* **2023**, No. e202301906.
- (26) Xu, W. C.; Sun, S.; Wu, S. Photoinduced Reversible Solid-to-Liquid Transitions for Photoswitchable Materials. *Angew. Chem., Int. Ed.* **2019**, *58* (29), 9712–9740.
- (27) Baroncini, M.; d'Agostino, S.; Bergamini, G.; Ceroni, P.; Comotti, A.; Sozzani, P.; Bassanetti, I.; Grepioni, F.; Hernandez, T. M.; Silvi, S.; Venturi, M.; Credi, A. Photoinduced Reversible Switching of Porosity in Molecular Crystals Based on Star-shaped Azobenzene Tetramers. *Nat. Chem.* **2015**, *7* (8), 634–640.
- (28) Akiyama, H.; Kanazawa, S.; Okuyama, Y.; Yoshida, M.; Kihara, H.; Nagai, H.; Norikane, Y.; Azumi, R. Photochemically Reversible Liquefaction and Solidification of Multiazobenzene Sugar-alcohol Derivatives and Application to Reworkable Adhesives. *ACS Appl. Mater. Interfaces* **2014**, *6* (10), 7933–7941.
- (29) Hoshino, M.; Uchida, E.; Norikane, Y.; Azumi, R.; Nozawa, S.; Tomita, A.; Sato, T.; Adachi, S.; Koshihara, S. Y. Crystal Melting by Light: X-ray Crystal Structure Analysis of an Azo Crystal Showing Photoinduced Crystal-melt Transition. *J. Am. Chem. Soc.* **2014**, *136* (25), 9158–9164.
- (30) Bleger, D.; Dokic, J.; Peters, M. V.; Grubert, L.; Saalfrank, P.; Hecht, S. Electronic Decoupling Approach to Quantitative Photoswitching in Linear Multiazobenzene Architectures. *J. Phys. Chem. B* **2011**, *115* (33), 9930–9940.